AFRL-RV-PS-
TR-2014-0021

TEMPERATURE INSENSITIVE AND RADIATION HARD PHOTONICS

Luke Lester and David Murrell

University of New Mexico
1700 Lomas Blvd NE
Albuquerque, NM 87106-3807

19 Mar 2014

Final Report

AIR FORCE RESEARCH LABORATORY
Space Vehicles Directorate
3550 Aberdeen Ave SE
AIR FORCE MATERIEL COMMAND
KIRTLAND AIR FORCE BASE, NM 87117-5776

DTIC COPY
NOTICE AND SIGNATURE PAGE

This report is the result of contracted fundamental research deemed exempt from public affairs security and policy review in accordance with SAF/AQR memorandum dated 10 Dec 08 and AFRL/CA policy clarification memorandum dated 16 Jan 09. This report is available to the general public, including foreign nationals. Copies may be obtained from the Defense Technical Information Center (DTIC) (http://www.dtic.mil).

AFRL-RV-PS-TR-2014-0021 HAS BEEN REVIEWED AND IS APPROVED FOR PUBLICATION IN ACCORDANCE WITH ASSIGNED DISTRIBUTION STATEMENT

//SIGNED//
STEVEN A. LANE
Program Manager

//SIGNED//
PAUL HAUSGEN
Technical Advisor, Spacecraft Component Technology Branch

//SIGNED//
BENJAMIN M. COOK, Lt Col, USAF
Deputy Chief, Spacecraft Technology Division
Space Vehicles Directorate

REPORT DOCUMENTATION PAGE

Form Approved
OMB No. 0704-0188

1. REPORT DATE *(DD-MM-YYYY)*	**2. REPORT TYPE**	**3. DATES COVERED** *(From - To)*
19-03-2014	Final Report	30 Nov 2011 to 28 Feb 2014

4. TITLE AND SUBTITLE

TEMPERATURE INSENSITIVE AND RADIATION HARD PHOTONICS

5a. CONTRACT NUMBER
FA9453-12-1-0132

5b. GRANT NUMBER

5c. PROGRAM ELEMENT NUMBER
62601F

6. AUTHOR(S)

Luke Lester and David Murrell

5d. PROJECT NUMBER
4846

5e. TASK NUMBER
PPM00013409

5f. WORK UNIT NUMBER
EF006716

7. PERFORMING ORGANIZATION NAME(S) AND ADDRESS(ES)

University of New Mexico
1700 Lomas Blvd NE
Albuquerque, NM 87106-3807

8. PERFORMING ORGANIZATION REPORT NUMBER

9. SPONSORING / MONITORING AGENCY NAME(S) AND ADDRESS(ES)
Air Force Research Laboratory
Space Vehicles Directorate
3550 Aberdeen Ave SE
Kirtland AFB, NM 87117-5776

10. SPONSOR/MONITOR'S ACRONYM(S)
AFRL/RVSV

11. SPONSOR/MONITOR'S REPORT NUMBER(S)
AFRL-RV-PS-TR-2014-0021

12. DISTRIBUTION / AVAILABILITY STATEMENT

Approved for Public Release; distribution is unlimited.

13. SUPPLEMENTARY NOTES

14. ABSTRACT

This investigation examines the durability of the Quantum Dot Mode-Locked Laser (QDMLL) for use in extreme environments where ionizing radiation is a threat. These QDMLLs are fabricated using dots-in-a-well (DWELL) epitaxial structures, which utilize the unique properties of 2D and 3D quantum structures to achieve low-threshold current density in an exceptionally durable gain medium. The research at the University of New Mexico summarized in this report details the radiation hardness of the mode-locking characteristics of the lasers themselves. We show that the devices tested continue to perform well even after being dosed with sufficient ionizing radiation to simulate a long mission at geostationary orbit altitudes.

15. SUBJECT TERMS

Space communication; satellite communication; quantum dot laser; photonics

16. SECURITY CLASSIFICATION OF:			**17. LIMITATION OF ABSTRACT**	**18. NUMBER OF PAGES**	**19a. NAME OF RESPONSIBLE PERSON**
a. REPORT	**b. ABSTRACT**	**c. THIS PAGE**			Steven A. Lane
Unclassified	Unclassified	Unclassified	Unlimited	28	**19b. TELEPHONE NUMBER** *(include area code)*

(This page intentionally left blank)

TABLE OF CONTENTS

LIST OF FIGURES

ACKNOWLEDGMENTS

This material is based on research sponsored by Air Force Research Laboratory under agreement number FA9453-12-1-0132. The U.S. Government is authorized to reproduce and distribute reprints for Governmental purposes notwithstanding any copyright notation thereon.

DISCLAIMER

The views and conclusions contained herein are those of the authors and should not be interpreted as necessarily representing the official policies or endorsements, either expressed or implied, of Air Force Research Laboratory or the U.S. Government.

(This page intentionally left blank)

1 SUMMARY

This investigation examined the durability of the Quantum Dot Mode-Locked Lasers (QDMLL) for use in extreme environments where ionizing radiation is a substantial threat. Mode-Locked lasers generate a train of optical pulses that have very narrow temporal width, making them useful for digital communications. These QDMLLs were fabricated using Dots-in-a-Well (DWELL) epitaxial structures, which utilized the unique properties of two-dimension (2D) and three-dimension (3D) quantum structures to achieve low-threshold current density in an exceptionally durable gain medium. QDMLLs are well suited to mode-locking because of the very high differential gain resulting from their one-dimensional (1D) quantum geometry. Research at the University of New Mexico summarized in this report details the radiation hardness of the mode-locking characteristics of the lasers themselves. We show that the devices that were tested continued to perform well, even after being dosed with sufficient ionizing radiation to simulate a long mission at geostationary orbits. The QDMLL is an exceptionally radiation hardened device with potential application for use in optical backplanes of on-orbit space vehicles.

2 INTRODUCTION

System durability is the enduring focus of any design engineer that seeks to meet the bandwidth demand challenges in the future. New control and communications systems that use photonics to relieve the crushing bandwidth demands must be robust enough to survive the extreme environments where they must function. The outer reaches of our atmosphere and beyond comprise the harshest environments known. Valid orbits from the rapidly traversing low Earth orbit (LEO) to the relay standby of geosynchronous Earth orbit (GEO) all have extreme variations in temperature and other hazards.

Exposure to ionizing radiation is a constant threat beyond the confines of Earth's atmosphere. Much effort has been devoted to mapping the magnitude and geography of these threats in orbit by research groups from around the world. Direct experimental measurements aboard manned fights at lower altitude and geostationary satellites have been performed for years. Experimental data from a geostationary satellite using radiation sensitive transistors characterized the yearly dose measured in 2003 [1]. This is the orbit that communication satellites would most likely inhabit. Bhat's experiment on the Geostationary Satellite (GSAT)-2

orbiter employed a series of radiation-sensitive elements with aluminum shielding varying from less than 1-mm in thickness to that approaching 1-cm. Their calculated yearly radiation dose for moderate shielding was less than 1-krad per year.

Radiation caused by solar activity follows a cyclic pattern with spurts of activity resulting from sunspots and flares. This pattern has been well studied also, which means that we can examine solar activity from 2003 GSAT-2 data to determine potential maxima. Examination of solar activity for that time period reveals that 2003 was a moderate year for solar radiation sources [2]. Thus, the measurements on the GSAT-2 spacecraft provide an excellent *baseline* for anticipating what our devices could be expected to see in space (i.e., a nominal radiation environment).

Extremes of ionizing radiation do not reflect the only environmental challenge that orbital vehicles must endure. Temperature variations are extreme between the sides of the spacecraft illuminated by sunlight and those left in the dark. The reliability of devices over temperature is of particular interest in any well-conceived durability study. Furthermore, thermal challenges are not so alien to us here within the atmosphere and many techniques from radiators to Peltier electric regulators have been developed to manage them. In space, many of these solutions are effective and require one currency to function, that being power. Energy generated by a spacecraft is preciously finite and any savings in power allowed by wider envelopes of temperature operation are a welcome addition to any systems engineer tasked with power balancing.

The QDMLL has shown exceptional resilience in regard to operating temperature. Devices under test have been operated at temperatures exceeding 100 °C, and their wall-plug efficiency increases as their temperature cools [3]. The wall plug efficiency is a direct measure of the conversion from input electrical energy to output optical photons. Reliability in these two extremes of temperature and ionizing radiation make the QDMLL ideally suited for operation aboard an orbiting vehicle as part of a communications system.

2.1 Ultra-fast Optical Networking

The concept of an ultra-fast network on chip, using assorted multiplexing methods, has been well-implemented in fiber optic telecommunications systems. The rush to develop fiber with the appropriate material properties took up much of the 1990’s and remains well-

implemented to this day. The reason for substituting optical communications for copper waveguides still holds for changing the backplane of orbiters today; higher bandwidth is possible using a smaller cable when optical techniques are employed. This is due to several unique properties of light, and its conduits that make it an ideal communications medium.

First, the frequency of light far exceeds that of microwaves, which allows for a much higher data bandwidth. Additionally, light of different wavelengths can travel along the same waveguide while maintaining the information each color (i.e., wavelength) channel contains. This allows for many additional channels to be used in parallel along the same connecting channel. This technique is known as wavelength division multiplexing (WDM). Lastly, laser sources can be made to deliver frequency-stable pulses of light through mode-locking using various techniques. These pulses range between femtoseconds to nanoseconds in temporal width depending on the method used. These pulse-trains can be multiplexed in time, creating a new pulse-train that can carry data at integer multiples of the laser's initial mode-locking repetition rate. Multiplexing in time, independent of wavelength, is known as optical time division multiplexing (OTDM).

Optical time division multiplexing allows for an additional method to increase the bandwidth of WDM techniques. A sample system based on passive delay lines constructed by our colleagues at the Rochester Institute of Technology is shown in Figure 1 [4]. This system is used to split one pulse into many by offsetting optical pulses using variable delay lines. The optical signals coupled into the system pictured in Figure 1 travel along the four waveguide paths with each circular section representing an optical delay path of equal length. Thus, the optical pulse that enters the OTDM multiplexer will be copied and time-shifted so that the output appears to be an integer multiple of the initial repetition rate. That integer will be equal to the number of independent optical paths available in the multiplexer. In the case of Figure 1, the frequency multiplication is a factor of four.

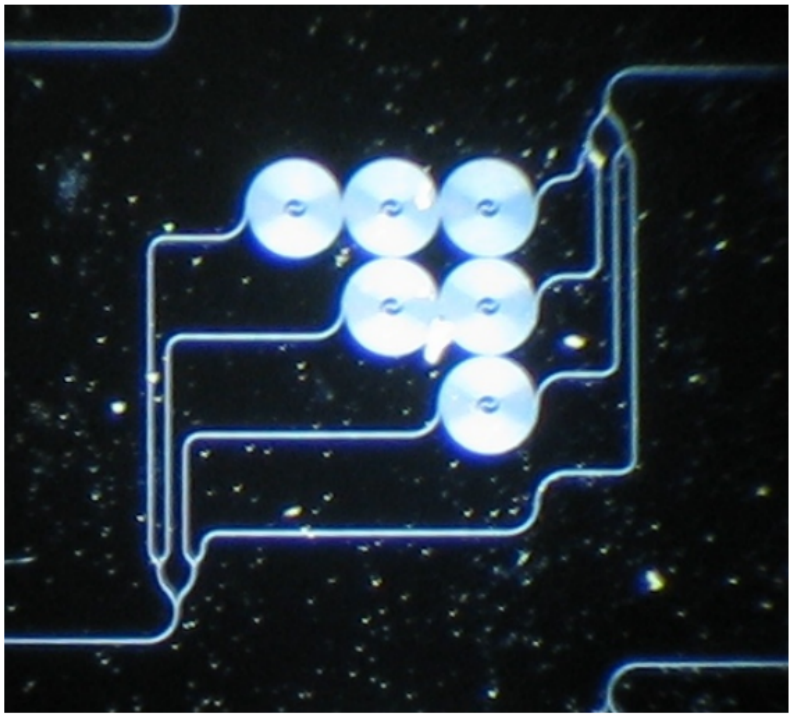

Figure 1. OTDM Pulse Multiplexer for Increasing the Output Repetition Rate Signal

Integration of an optical modulator, like the ring resonators described later in this section [5, 6], into the OTDM setup in Figure 1 allows for the transmission of binary information at a repetition rate of the input laser. This is done by increasing the loss on one of the waveguide paths electrically using the ring resonator. This would *darken* one of the pulses in the output multiplexed train, allowing for the communication of binary data. For example, if the input repetition rate of the laser was 10 GHz, then the pictured OTDM setup would create an equivalent pulse train with a repetition rate of 40 GHz. Limitations of this increase in repetition rate are found in the total-loss-per-unit-length of the waveguide and the input pulse width. The number of channels can be increased so long as the attenuation from the waveguide does not mute the input pulses, and the temporal spacing of the pulses in the output is greater than the initial pulse width. The advantage of this system is that the modulators operate at the frequency of the laser and not at the eventual data rate. Data is multiplexed to create an effective transmission that is higher than the laser pulse rate, but modulation of each input channel only requires oscillators operating at the same frequency of the laser's pulse train. In the case of the

example in Figure 1, this means that an active system following the same geometry would require resonators only 1/4 the speed of the output data transmission. This means that lower power modulators that operate at slower frequencies can be substituted at a savings in weight and power requirements. WDM operations applied to this allow for additional channels on top of the OTDM system. These channels are separated by color (i.e., wavelength). Thus, even more data can be transmitted along the same waveguide when WDM techniques are applied in concert with OTDM.

For completeness, this conversation must include a comment on WDM setups. We do not currently have access to WDM modulating ring resonators, but preparations for this technology must also be considered in this study. Modulation techniques can be applied to semiconductor waveguide systems using tunable ring resonators grown on silicon [5]. These devices have the ability to electrically shift their resonant wavelength at high speed. High speed and high resonator quality means that these rings can operate as switches for data communication by picking off wavelengths of interest. Collaborations with the University of Rochester and Rochester Institute of Technology have given us insight into these systems.

A schematic diagram of a hypothetical WDM system using ring resonators is shown in Figure 2 [7]. The 90-degree bends in the waveguide structure do not couple well without the use of the ring resonator. Broad light sources, represented by the white arrow, can be partitioned into their component colors using active ring resonators. When these rings are active, light will couple into the perpendicular waveguide and reduce the intensity of that light along the main optical channel. This allows for a Boolean communication of data using on and off settings. The resonance peak of each ring pictured in Figure 2 is relative to the size of that ring, in addition to the electrical bias on it. Such a system provides the basic method for communicating binary data along multiple independent channels separated by wavelength. These technologies are state-of-the-art, and variations of the electrically tunable ring resonator are being tested all over the country. Individual modulators have been demonstrated as thermally tunable and quick responding. State-of-the-art resonators can achieve modulation frequencies beyond 12.5 GHz. This means that the WDM techniques can transmit data at least at 12.5 Gb/s for each color channel. Combination of this technique with OTDM could expand the transmitted data bandwidth even further.

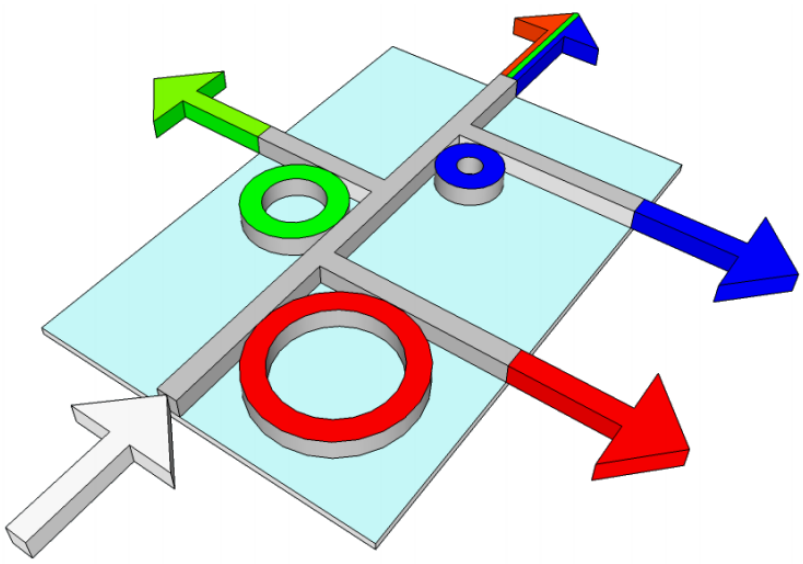

Figure 2. WDM Functional Illustration Showing the Isolation of Data Channels by Wavelength

2.2 Quantum Dot Mode-Locked Laser

The multiplexing technologies in the previous section require a light source to make all of these elements function. The ideal source for providing the necessary optical signal for the above networking techniques is a mode-locked laser. These lasers use internal modulation of the elements inside of the optical cavity to generate a continuous train of short pulses. As described in the Introduction, these pulses vary in width and repetition rate based on the method used to create them. There are two basic schools of mode-locking that are employed independently or in hybrid configurations. The first school is active mode-locking. This requires that an external high frequency source be used to create the pulse train, which must be synchronized and carefully monitored. The technique requires extensive RF generating equipment and is highly sensitive to temperature and other instabilities. All of the components to such an active mode-locking setup utilize a large amount of weight and power. However, this technique allows for the shortest possible pulses at a cost of increased complexity.

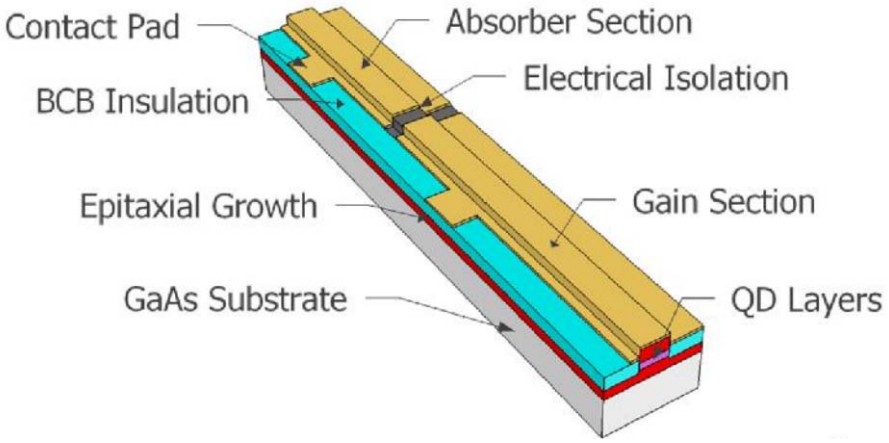

Figure 3. Two Section QDMLL Device Schematic

Passive mode-locking is the other school to achieve short pulses, and is the technique of choice for the optoelectronics group at the University of New Mexico. These devices use a nonlinear element called a *saturable* absorber, which is used to generate a mode-locked pulse train without external modulation. A monolithic III-V semiconductor configuration of GaAs can produce a mode-locked laser, like the one in Figure 3, without the need for radio frequency equipment required to maintain active mode-locking. A complex system requiring extensive power and heat dissipation can be replaced with a single semiconductor merely millimeters in length. Operation of this laser requires only direct current (DC) voltages in the most basic of implementations. One section of the semiconductor serves as the laser gain, and the other as a mode-locking element, the *saturable* absorber. A schematic diagram of a horizontally emitting semiconductor laser is shown in Figure 3. Each section is electrically isolated to allow for independent gain and saturable absorption regions. The ridge waveguide is coated with a metal contact, which allows direct integration into electrical systems for ease of use. Emission of light is along the waveguide facet, which can be coupled into optical fiber or into silicon modulators for data multiplexing.

The examination of the Quantum Dot Mode-Locked Laser (QDMLL) as a potential for a light source useful in an optical backplane on flight vehicles performed by the University of New Mexico has been aided by the fitness of the QDMLL for the task. The laser structure needed for this research was identified and interrogated for temperature independence. The construction of

this device is of particular interest because physical properties of the gain producing layer make it more resilient when exposed to ionizing radiation.

The active region of the two-section QDMLL is comprised of 6-stacks of InAs quantum dots in an InGaAs quantum well, the so-called DWELL structure. These layers are separated by GaAs barriers grown by elemental-source molecular beam epitaxy (MBE). This growth technique allows for precise control of elemental composition as well as finite precision in layer thickness. An illustration showing the cross-sectional layout of the QDMLL is given in Figure 4. The center of the DWELL technology lies in the technique to create self-assembling layers populated by *islands* of InAs semiconductor material. These islands are small enough to exhibit 3D quantum confinement, which is why they have earned the moniker of *Quantum Dot*. They are formed by a unique effect born of lattice mismatch between the different crystalline structures of GaAs and InAs. The active layers that generate the optical gain are highlighted in purple in Figure 4. The two bounding layers buffering the gain region act as the optical waveguide boundaries as well as strain mitigation. A low step index, 30% AlGaAs cladding, facilitates high power operation by reduction of the optical confinement factor. All of these parameters address the gain material of the laser but only in cross-section. A functional device has a finite length to create a lasing cavity. The selected length defines the mode spacing, intrinsic passive repetition rate, and threshold current required to operate the device. Figure 4 also shows an atomic-force microscope (AFM) image of an individual quantum dot (QD) layer.

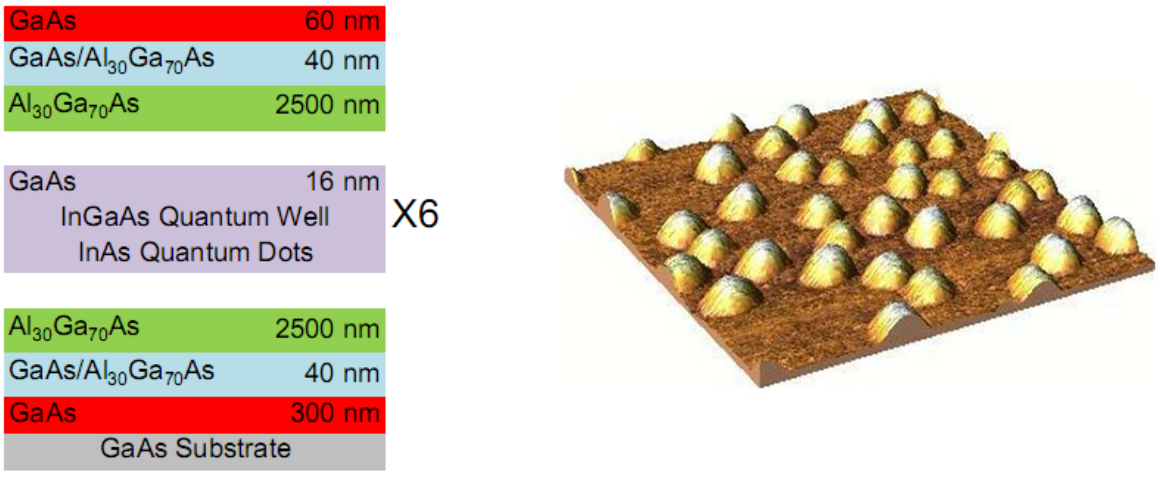

Figure 4. QDMLL Laser Structure and AFM Image of an Individual QD Layer

Final dimensions for the lasing bar are 0.3-mm in width, and 8.0-mm in length. The 8.0-mm laser cavity length produces a pulsed laser output with a 200-ps pulse interval. This corresponds to a repetition rate of 5 GHz. The facets are high-reflection (HR) (95%) / anti-reflection (AR) (5%) coated. The absorber is adjacent to the HR coated facet, which creates a colliding pulse mechanism to improve pulse trimming. The lasers operate with a center wavelength of approximately 1310-nm at room temperature. These lasers are then mounted on AlN carriers for mechanical rigidity and thermal conductivity, as shown in Figure 5. This material also provides a position for external wiring and allows for the addition of thermistors for temperature control near the lasers. All of these, in the compact package, have a launch weight of less than a gram. These mounted devices have been used to characterize the properties of this family of QDMLLs. These are the devices that will be tested in irradiation. A low-jitter source of optical pulses with small size and low weight are well-suited for flight applications, which are always conscious of reliability and launch mass.

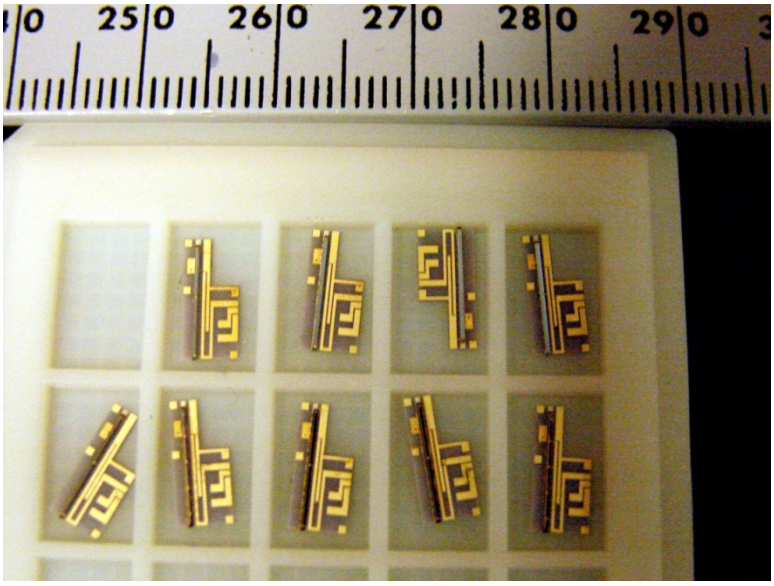

Figure 5. The Sample Set of QDMLL's for Temperature Independence Studies and Radiation Hardness Testing in their Transport Container

3 METHODS, ASSUMPTONS, AND PROCEDURES

The fundamental method of analysis used in this study was the comparison of device modal gain, which can be used to predict device operation as well as mode-locking conditions. The laser used in this test was examined for its device modal gain as well as the pulse characteristics at various bias conditions. These benchmarks were achieved using the segmented contact method. The damage behavior was modeled based on temperature performance estimates. These tests were performed again after the irradiation session and the results recorded. Temperature variation tests using the segmented contact method produced data used in predictive models.

3.1 Gain and Loss Characteristics

A temperature dependent picture of the gain profile of our quantum dot laser devices is critical to our prediction of the device properties. To this end, a measurement setup was devised that had the capability to perform data sampling at the full range of temperatures required for this work. Currently, this setup is capable of temperature ranges from 10 °C to 40 °C, with the intention to complete the final expansion to full temperature capacity. The system was designed with a very high thermal mass near the laser itself to maintain equilibrium temperature during each of these current measurements. The schematic diagram of the experimental setup is given in Figure 6. The device was comprised of 11 electrically isolated sections with dimensions of 0.5-mm x 0.0035-mm. The gain sections were comprised of two device sections, making the total length of each 1-mm. The remainder of the device length was used as an absorber to reduce back-reflections.

Electronic control is presently done using an electronic control board that was re-purposed from previous work at University of New Mexico (UNM). Two current sources and a voltage source were used to stimulate the device. Measurements were conducted using an integrating-sphere power meter and an Agilent spectrometer. Data capture was performed via (general purpose interface bus) GPIB connections to a central computer. Coupling of the laser light from the quantum-dot laser was achieved through an integrated optical head containing a small lens and isolator. This head coupled the light into a fiber, which was routed to the measurement equipment. The coupling lens was AR coated to reduce back-reflections.

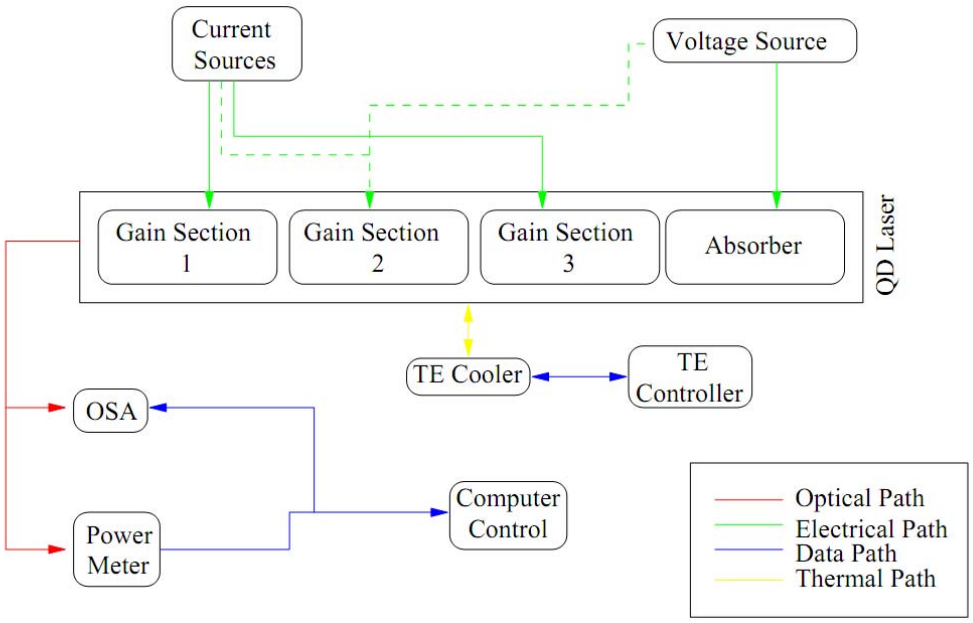

Figure 6. Segmented Contact Measurement Setup More Measurement of Laser Gain

The theory behind the segmented contact gain measurement method was taken from previously published work [8]. Our measurement method required single-pass amplification of spontaneous emission of the gain sections shown in Figure 6. The expression for computing the net modal gain of the laser is given by the following equation:

$$g = ln\left(\frac{I_3 - I_1}{I_2 - I_1} - 1\right) L^{-1}, \quad (1)$$

where I_x indicates the intensity from each of the three measurement steps, and L is the length of the gain sections. Absorption measurements were arrived at using a similar technique with the following expression:

$$g = ln\left(\frac{I_2 - I_1}{I_4 - I_1} - 1\right) L^{-1}, \quad (2)$$

where the variables follow the abovementioned convention. Further detail of this method can be found in the published literature.

We can now proceed to the results as a function of temperature or radiation damage by looking at differences. The last piece of information that can be gleaned about the laser is the value of the internal loss of the cavity. The convergence point for the gain measurement data at lower wavelength is a representation of the internal loss of the cavity in units of inverse cm (i.e.,

cm^{-1}). This is a measure of the loss in the optical waveguide as an aggregate of all obstructions and imperfections, and provides an excellent method for assessing viability.

3.2 Irradiation and Experimental Methods

Previous experiments with QDMLL's have shown that they can operate while under gamma radiation, even after exposures as high as 120 Mrad. This provides an excellent backstop for our test, because such dosages are well beyond what is proposed in this investigation. On-orbit exposure observed at geostationary altitude averages about 3.4 krad per year. One must also consider the effects of periodic solar flares, which would increase the radiation dosage. Worst-case estimates for dosages on orbit have been calculated from historical events. Expectations for the largest feasible solar events could add an additional 1.5 krad for a satellite in the most susceptible polar orbits. Two devices were selected for irradiation. First was a device selected because of its usefulness to gain profile measurements using the segmented contact method. The second device was a working laser that can be used to test the effect of irradiation on the mode-locking pulses of the laser itself.

Characterization of both devices used in the irradiation test was completed to provide a baseline temperature and electrical response. One irradiation session of 2.2 Mrads from a ^{60}Co source has been performed, which would correspond to average flight duration of several *centuries*. This provides an excellent reliability standard for integration into any system, and provides an exceptionally high ceiling for radiation bursts. These burst of radiation from solar events or of cosmic origin can greatly exceed the average exposure values. Analysis of the gain and loss curves of the diagnostic devices after the irradiation will provide us with the metrics that we can use to gauge the overall effect of the radiation damage.

The testing facility was the ^{60}Co irradiation facility at the Air Force Research Laboratory in Albuquerque, NM. This highly energetic source allowed us to examine the behavior of the device after a significant radiation dose. Verification of mode-locked operation after the irradiation set was satisfactory to confirm the hardness of the device. Mode-locked operation was verified through the use of a high-speed digitizing oscilloscope and an optical auto-correlator. Further characterization of the thermal characteristics of the lasers themselves allowed us to determine a full range of the mode-locking capability, even after irradiation far beyond what would be expected in an actual operational flight.

4 RESULTS AND DISCUSSION

Characterization of the two lasers used in the study began with a gain and loss measurement characterization across a broad temperature range over the entire emission bandwidth. The multi-section laser was used for this purpose, because its evenly divided sections allowed for the execution of the segmented contact method as previously discussed. Gain and loss data were taken for 20, 40, 60, 80, 100, 110 and 120 °C. This reveals the absolute gain profile as the laser warms. The gain curve of the laser becomes informative in the full range of mode-locking possibilities. The information presented in Figure 7 provides the basic operation characteristics of the laser, which we can use to extract the idealized mode-locking regimes.

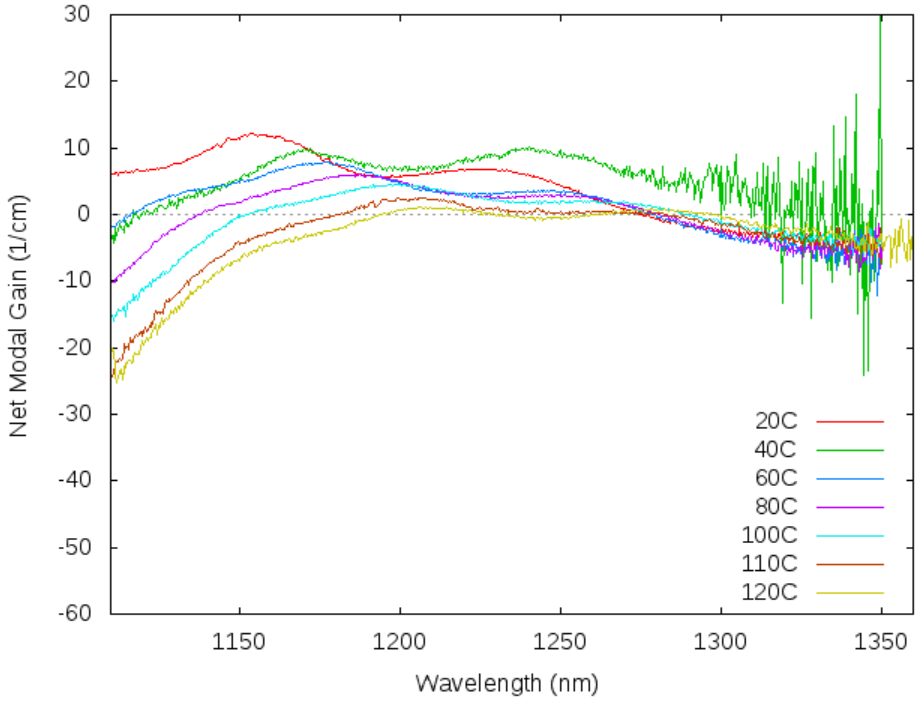

Figure 7. Gain Profile Measurements at Constant Current Density Over Temperature

Using the following expressions, we show the predicted range of mode locking:

$$\frac{L_a}{L_g} > \left(\frac{\frac{dg_0}{dJ}}{\frac{dg_0}{dJ}|_{g_0=0}}\right)^2 \frac{g_0(J)}{a_0}, \text{ and} \tag{3}$$

$$\frac{L_a}{L_g} = \frac{g_0(J)-\alpha_m-\alpha_i}{a_0+\alpha_m+\alpha_i}, \tag{4}$$

where J is current density, L are length measurements, g is the gain value, and α are the absorption values of the laser. The former expression defines the minimum mode-locking condition, which provides a lower bound to the operational current density of the laser. The second equation is the lasing threshold condition, which determines the upper bound of the absorption values permissible for the laser to operate. This is all framed in terms of the absorber and gain length ratios, which consider the physical length of the two parts on the laser itself. These pieces were shown earlier in Figure 3.

The results of these computations were then plotted into a series of concentric curves. The regions within these curves indicate device configurations deemed suitable for mode-locking operations. Detailed analysis of lasers with multiple examples of the absorber / gain length ratio has proven this model to be robust in its predictions.

The expected mode-locking range for our device from the multi-section prediction is shown in Figure 8. The enclosed regions of the curve again indicate regions of expected mode locking. Plotted lines indicating different hypothetical devices with varying absorber lengths help illustrate how a single device can operate in a mode-locking regime over a wide temperature range. Explicitly, a laser configuration can exhibit mode-locking operation for a wider temperature range as more enclosed regions are traversed by the horizontal line representing it.

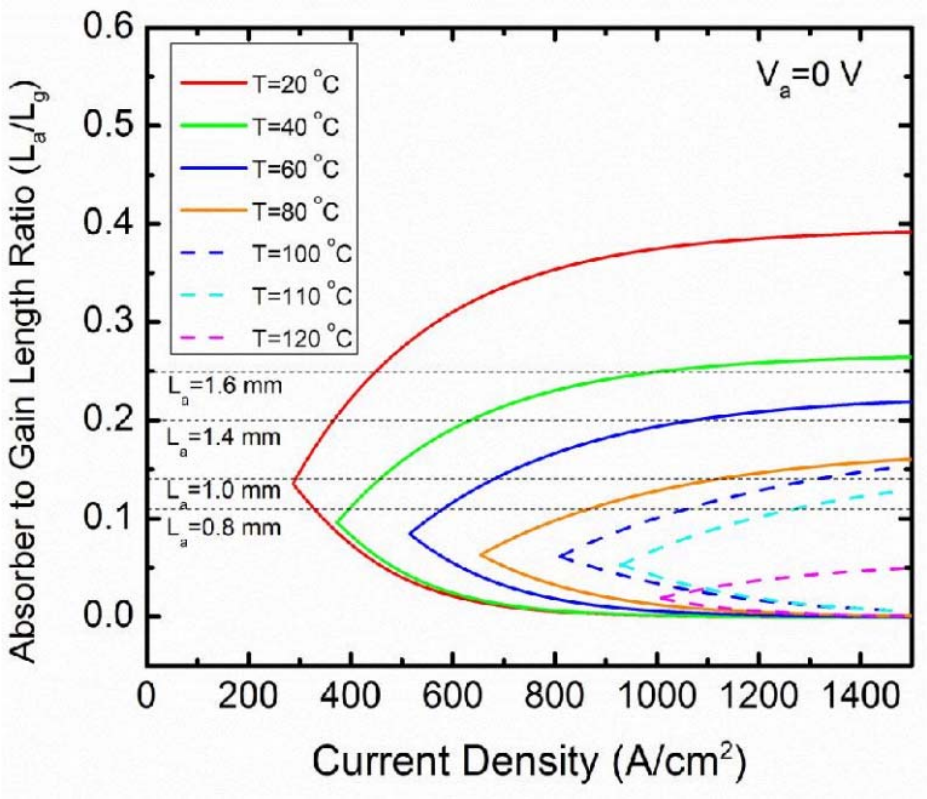

Figure 8. Predicted Mode Locking Range for the QDMLL

We then turned our attention to the second device under test, which was a more traditional 2-section laser. We developed a measurement scheme to sample the laser over a wide range of biasing parameters to examine the boundaries to mode-locking. We found excellent agreement with the model and verified that our QDMLLs can operate over a broad range of conditions as shown in Figure 9.

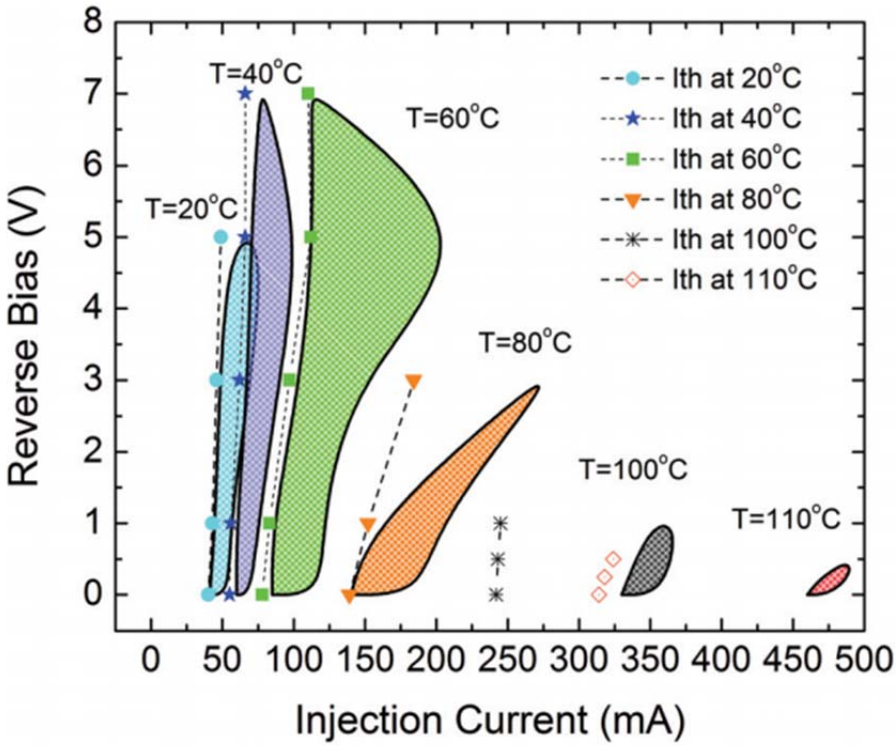

Figure 9. Observed Mode Locking for the QDMLL

5 CONCLUSIONS

Results for the temperature dependent mode-locking analysis on the family of QDMLLS under test were promising. Temperature studies showed that there was suitable mode-locking operation for observed pulses for temperatures as high as 120 °C and as low as 20 °C. Analysis of QDMLLS operating over this broad range produced stable mode-locking over the full range. Investigations into the QDMLLs at higher temperature showed the upper operational bounds continue to increase to hotter regimes. Irradiation of two QDMLL samples with a dose that far exceeded expected on-orbit requirements was completed without destroying the devices under test. This result was a reinforcement of previous work that dealt only with lasing threshold degradation as a function of applied radiation dose. We suspect that the partitioned nature of the gain material, consisting of many quantum dots, is less susceptible to radiation damage as destruction of a few of these dots does not significantly impact the performance of the device as a whole.

Broad-scale analysis of these parameters provided us the baseline for comparison to evaluate the health of these devices after the irradiation set was completed. Initial device testing has shown that mode-locking is possible after the irradiation, but the extent of the damage has not yet to be quantified, because the lasers were not tremendously harmed by the irradiation set.

This technology provides excellent promise for integration into systems that operate in environments of high radiation hazards and wider temperature conditions. The durability benefit is compounded by the compact size and low mass of these devices, and the equipment necessary to control them. These devices are remarkably radiation hard, and deserve further investigation for integration into next generation communications systems in extreme environments.

6 RECOMMENDATIONS

Post-irradiation measurements of these lasers were done selectively, rather than attempt to reproduce the entire map. As expected, the lasers continued to be able to mode-lock even after bombardment with 2.2 MRads of ionizing radiation from a ^{60}Co source. Further investigation is required over a longer irradiation period to determine the precise failure condition of these lasers.

REFERENCES

1. B. Bhat, N. Upadhyaya, and R. Kulkarni, “Total Radiation Dose at Geostationary Orbit,” *IEEE Transactions on Nuclear Science*, 52(2):530–534, April 2005.

2. G. Reitz and Guenther Reitz Ã., “Characteristic of the Radiation Field in Low Earth Orbit and in Deep Space,” *Zeitschrift für Medizinische Physik*, 18(4):233–243, December 2008.

3. J. K. Mee, M. T. Crowley, N. Patel, D. Murrell, R. Raghunathan, A. Aboketaf, A. Elshaari, S. F. Preble, P. Ampadu, and L. F. Lester, “110 °C Operation of Monolithic Quantum Dot Passively Mode-Locked Lasers,” *2012 23rd IEEE International In Semiconductor Laser Conference* (*ISLC*), San Diego, CA., pp. 68–69.

4. Abdelsalam A., A. Elshaari, and S. Preble, “Optical Time Division Multiplexer on Silicon Chip,” *Opt. Express*, 18(13):13529–13535, June 2010.

5. P. Dong, R. Shafiiha, S. Liao, H. Liang, N. Feng, D. Feng, G. Li, X. Zheng, A. Krishnamoorthy, and M. Asghari, “Wavelength-Tunable Silicon Micro Ring Modulator,” *Opt. Express*, 18(11):10941–10946, May 2010.

6. R. Soref, “The Past, Present, and Future of Silicon Photonics,” *IEEE Journal of Selected Topics in Quantum Electronics*, 12(6):1678–1687, November 2006.

7. B. Jalali, M. Paniccia, and G. Reed, “Silicon Photonics, *IEEE Microwave Magazine*, 7(3):58–68, June 2006.

8. Y. Xin, Y. Li, A. Martinez, T. Rotter, H. Su, L. Zhang, A. Gray, S. Luong, K. Sun, Z. Zou, “Optical Gain and Absorption of Quantum Dots Measured Using an Alternative Segmented Contact Method,” *IEEE Journal of Quantum Electronics*, 42(7):725–732, July 2006.

LIST OF SYMBOLS, ABBREVIATIONS AND ACRONYMS

1D	One Dimension
2D	Two Dimension
3D	Three Dimension
^{60}Co	Radioactive cobalt, isotope 60
AFM	Atomic Force Microscope
AlGaAs	Aluminum Gallium Arsenide
AlN	Aluminum Nitride
AR	Anti-Reflection
DC	Direct Current
DWELL	Dots-in-a-Well
GaAs	Gallium Arsenide
GEO	Geosynchronous Earth Orbit
GPIB	General Purpose Interface Bus
GSAT-2	Name of an experimental communications satellite built by the Indian Space Research Organization; assumed to stand for Geostationary Satellite revision 2
HR	High-Reflection
InAs	Indium Arsenide
InGaAs	Indium Gallium Arsenide
LEO	Low Earth Orbit
MBE	Molecular Beam Epitaxy
QD	Quantum Dot
QDMLL	Quantum Dot Mode-Locked Laser
OTDM	Optical Time Division Multiplexing
UNM	University of New Mexico
WDM	Wavelength Division Multiplexing

DISTRIBUTION LIST

DTIC/OCP 8725 John J. Kingman Rd, Suite 0944 Ft Belvoir, VA 22060-6218	1 cy
AFRL/RVIL Kirtland AFB, NM 87117-5776	2 cys
Official Record Copy AFRL/RVSV/Steven Lane	1 cy